



# Study of Neutron Capture Cross Sections by TOF Method

Oleg SHCHERBAKOV Hideo HARADA Kazuyoshi FURUTAKA  
Shoji NAKAMURA

Advanced Fuel Recycle Technology Division, Waste Management and Fuel Cycle Research Center, Tokai Works

中性子飛行時間計測法による中性子捕獲断面積の研究

オレグ・シェルバコフ 原田 秀郎 古高 和禎 中村 詔司

東海事業所 環境保全・研究開発センター 先進リサイクル研究開発部

サイクル機構で開発したBGO検出器とそのデータ収集系の性能を実証するために、 $^{237}\text{Np}$ の中性子捕獲断面積の測定を、1 1,000eVのエネルギー領域で行った。この検出器系は、16のセクションからなるBGO結晶を用いた全エネルギー検出器と、40MHzのflash ADCを用いたデータ収集システムからなっており、放射性核種による中性子捕獲断面積を飛行時間法で測定するために製作したものである。この検出器の応答関数、検出効率、ガンマ線及び中性子に対するエネルギー分解能及びバックグラウンド放射線量を、 $^{237}\text{Np}$ 及び $^{10}\text{B}$ の中性子捕獲断面積測定のためのテスト実験により測定し、計算による値との比較を行った。計算により得られた検出効率は、実験を通して得た値とよく一致していた。

*The neutron capture cross section measurements of  $^{237}\text{Np}$  have been carried out in the energy range 1 1,000 eV to demonstrate the performance of the new detector and data taking system developed at JNC. A 16 section BGO scintillation detector was used as a total energy detector in conjunction with the 40 MHz flash ADC. This detector system is intended for measurements of neutron capture cross sections of radioactive nuclei by the time of flight method. The detector response function, efficiency, gamma ray and neutron energy resolution, backgrounds were obtained through the test experiments to measure the neutron capture cross section by  $^{237}\text{Np}$  and  $^{10}\text{B}$ , and are compared with the results of calculation. The result of efficiency calculation agrees well with that obtained in the experiments.*

## キーワード

中性子吸収, 断面積, 実験, 飛行時間法, ガンマ線, BGO検出器, データ収集システム, ネプツニウム 237, 中性子エネルギー分解能, バックグラウンド

*Neutron Capture, Cross Section, Experiment, Time-of-Flight Method, Gamma Rays, BGO Detector, Data Taking System, Neptunium-237, Neutron Energy Resolution, Background*

## 1. INTRODUCTION

Neutron capture cross sections of long lived fission products and minor actinides have received much attention during last decade in the field of nuclear transmutation of radioactive waste. Accu-

rate measurement of these cross sections is a very difficult task, due to the high radioactivity of the samples under investigation. Among the various techniques used for capture cross section measurements, only a neutron time of flight (TOF)



オレグ・シェルバコフ

システム設計評価グループ  
核変換研究チーム所属  
国際特別研究員(ロシア, ベテ  
ルスブルグ原子核物理研究所)  
核変換技術開発のための基  
礎基礎データに関する研究  
に従事  
Ph.D



原田 秀郎

システム設計評価グループ  
核変換研究チーム所属  
サブグループリーダー 主任研究員  
核変換技術開発のための基  
礎基礎データに関する研究  
に従事  
理学博士, 第1種放射線取  
扱主任者



古高 和禎

システム設計評価グループ  
核変換研究チーム所属  
チームリーダー, 副主任研究員  
核変換技術開発のための基  
礎基礎データ  
及びその測定技術の高度化  
に関する研究に従事  
理学博士



中村 詔司

システム設計評価グループ  
核変換研究チーム所属  
副主任研究員  
核変換技術開発のための基  
礎基礎データに関する研究  
に従事  
理学博士, X線取扱主任者

method enables unique possibility to obtain data about energy dependence of the cross section in a wide energy range, from thermal (0.001–0.1 eV) up to tens of MeV, in a single measurement. A principle of the TOF method is explained in Fig.1.

A pulsed neutron source, usually driven by a high energy proton or electron accelerator, emits neutrons in short pulses having width in ns– $\mu$ s range. When neutron with energy  $E_n$  reaches a sample located at a distance  $L$  from the source, it is captured by one of the sample nuclei with mass number  $A$ . A compound nucleus  $A+1$ , formed in a highly excited state with excitation energy of  $B_n + E_n$  (where  $B_n \sim 5-10$  MeV is neutron binding energy), decays to its ground state by emitting a cascade of prompt capture  $\gamma$  rays. This event is registered by a gamma ray detector, which is located close to the sample. The neutron time of flight defined as a difference between  $t_1$  (a time of capture) and  $t_0$  (a time of production) is related with neutron energy  $E_n$  by a simple (in a non relativistic case,  $E_n < \text{few keV}$ ) equation:

$$t(\mu\text{s}) = \frac{\mu_0 L(m)}{\sqrt{E_n(eV)}} \quad (1)$$

where  $\mu_0 = 72.3$  is the TOF (in  $\mu\text{s}$ ) of a 1 eV neutron necessary to cover a distance of 1 m. By measuring TOF dependence of the detector counting rate, the energy dependence of the neutron capture cross section is obtained using the equation (1). A practical realization of the principle described above strongly depends on the properties of the applied detector and associated data taking

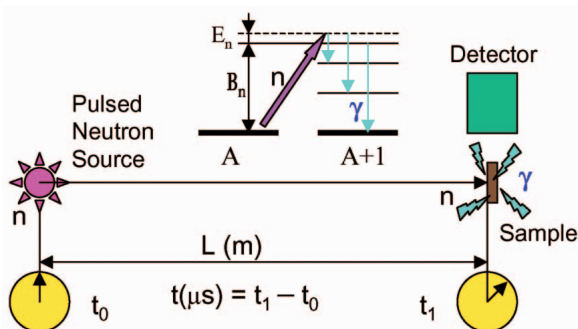


Fig. 1. Principal scheme of the neutron time-of-flight measurement.

system.

A detector of prompt gamma rays should have efficiency that is independent of spectrum shape and the multiplicity of the capture gamma ray cascades. One of the suitable detectors of this type is a large total energy absorption detector. The capture events registered by such detector give rise to pulse heights proportional to  $B_n + E_n$  that is constant with a good accuracy because  $B_n \gg E_n$ . Besides constant efficiency of registration of the capture event, a total absorption detector enables to separate unambiguously capture from natural background gamma rays (the latter usually have the energy much lower than  $B_n + E_n$ ). If large detector has a sectional structure, it can be also used as a gamma ray multiplicity spectrometer. This option can be effective in separating neutron capture from fission reaction, as well as for discriminating against background caused by neutrons scattered in capture sample.

Besides the capture gamma ray detector itself, another important part of the detector system that determines its experimental capabilities in TOF measurement is the data taking system. For the capture cross section measurements with highly radioactive samples, a problem of pulse pile up and count losses becomes very severe. It can be effectively resolved by applying a digital signal processing technique. With the development of modern high speed transient waveform recorders (flash ADCs), it becomes possible to carry out signal processing and acquisition in one unit combined with a conventional personal computer. Besides versatility of digital signal processing including a possibility of pulse shape analysis, this development has also simplified the data taking system by decreasing the number of electronic modules.

In the present report, the description of the large BGO detector and flash ADC based data taking system developed at the JNC is given, together with results of the test TOF measurements of neutron capture cross section of  $^{237}\text{Np}$ . The detector and associated data taking system are dedicated to the cross section measurements with

radioactive samples. This equipment is planned to be used in TOF measurements at the new generation high intensity pulsed neutron sources.

## 2. EXPERIMENTAL PROCEDURE

### 2.1 Experimental set up

A scheme of the measurements is shown in Fig. 2. The neutron beam was produced using the electron Linac of the Research Reactor Institute, Kyoto University (KURRI). Accelerated electrons struck a water cooled Ta target, producing fast neutrons having the evaporation spectrum with an average energy of  $\sim 0.7$  MeV. The slow neutrons were produced by moderating the fast neutrons in a 10 cm thick water moderator coupled with the neutron producing target. To decrease the overloading effect caused in the detector phototubes by intensive flash of gamma rays from the target, a lead shadow bar was used. It was placed on the neutron beam axis close to the neutron producing target, in such a way that the detector or sample under investigation do not "see" the target but only the moderator. The intensity of the neutron beam was monitored by the  $\text{BF}_3$  counter located in a gap between two sections of evacuated flight tubes.

The measurements of  $^{237}\text{Np}$  capture cross section in the neutron energy range 0.01 eV - 1,000 eV were performed at the following Linac operating conditions: the electron energy, 30 MeV; pulse

repetition rate, 20 - 100 Hz; pulse width, 47 ns - 3  $\mu$ s; and average electron current, 40 - 60  $\mu$ A.

A 24.2 m flight path equipped with evacuated flight tubes was used. The neutron beam was collimated to 50 mm diameter at the capture sample position by a set of lead, iron and  $\text{H}_2\text{BO}_3$  collimators. The BGO detector was shielded against external neutrons and gamma rays using lead blocks 5 - 10 cm thick. During the measurements, notch filters of Co, Mn, In, and Cd were put on the neutron beam to evaluate the background at various energy points. These points corresponded to the strong resonances in the total cross sections of these filter materials, for which the condition  $N_0 \times \sigma_0^{\text{tot}} \gg 1$  was fulfilled, where  $N_0$  is nuclear density and  $\sigma_0^{\text{tot}}$  is peak value of the total cross section corrected for energy resolution of the TOF spectrometer. Neutrons having corresponding energies were rejected by scattering or capture from the beam. The counts observed at the "bottom" of resonance dips corresponded to the events caused by background neutrons and gamma rays. The capture samples were set in the geometrical center of the detector. The parameters and design of the samples used in the measurements are shown in Fig. 3.

### 2.2 BGO detector

The capture gamma ray detector, shown in Fig. 4 and 5, consists of 2 identical halves, every one

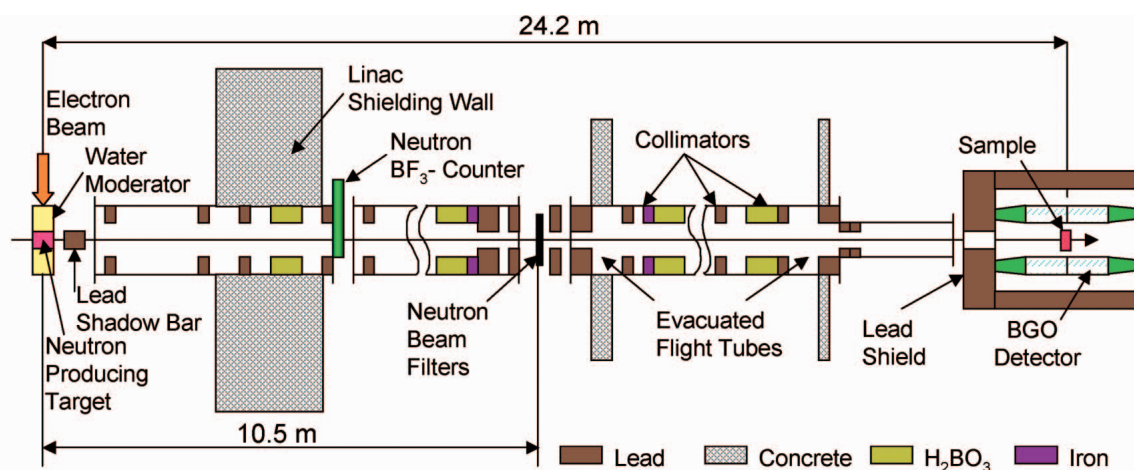


Fig. 2. Scheme of the neutron capture cross section TOF-measurement at the 24.2m flight path of the KURRI Linac.

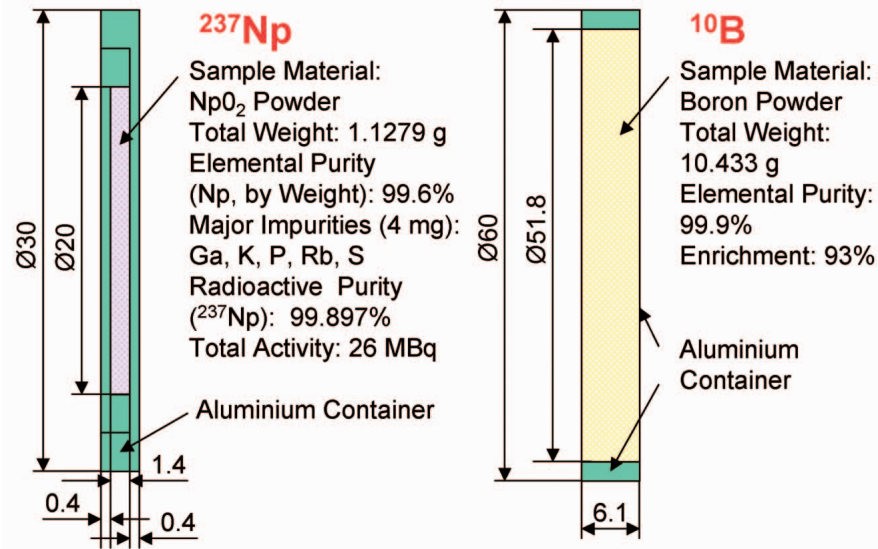


Fig. 3. Samples of <sup>237</sup>Np and <sup>10</sup>B, all dimensions are given in mm.

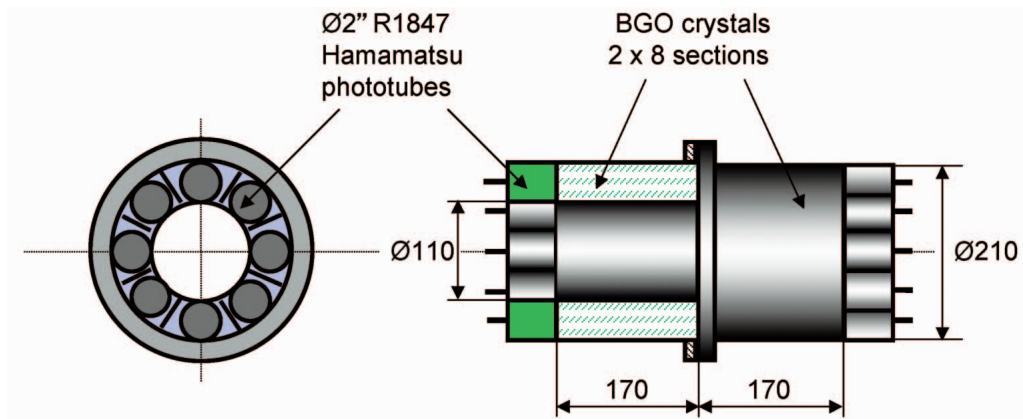


Fig. 4. BGO detector: front view (left) and side view (right) with a vertical cross section of one half.

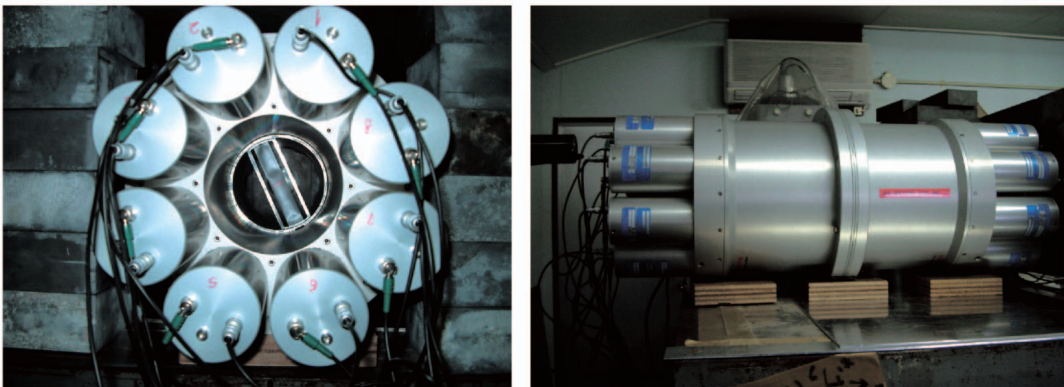


Fig. 5. Photograph of the BGO detector: on a front view (left) it can be seen aluminium frame (sample holder) and transparent acrylic film used for beam line adjustment by the laser.



containing 8 optically separated BGO (Bismuth Germanate Oxide) crystals 170 mm in length. These crystals form a cylindrical scintillator layer having internal and external diameters of 110 mm and 210 mm, respectively. The total volume of the detector scintillator is 8.54 liters. Every crystal is viewed by the  $\frac{1}{2}$ " Hamamatsu R1847 phototube. A total weight of the whole detector including structural materials is about 70 kg.

The major advantages of BGO are its very high density and the large atomic number of Bi component. The first feature enables construction of a detector of compact design. The large atomic number results in a high photoelectric absorption of gamma rays. Therefore, the probability of gamma ray re scattering (cross talk effect) from one section of the detector to another is considerably decreased.

### 2.3 Data taking system

A block diagram of the data taking system is shown in Fig. 6. The outputs of 16 photomultiplier tubes were combined into 2 groups and fed into two ORTEC 474 timing filter amplifiers. Then, after shaping and amplification, the signals were summed and inverted by the Tennelec TC253 unit and finally fed into a 40 MHz 4 channel 12 bit transient recorder PCI 412 (TRP 25). This flash

ADC board was installed in the 1.2 GHz PC (Dell, model Dimension 8200). In the course of time of flight measurements, a start signal for triggering the flash ADC ( $t_0$  timing mark) was generated by Linac electron pulse loaded on a Ta neutron producing target.

The pulses from the BGO detector were digitized into 25~250 ns time bins and temporarily stored in 2M buffer memory of the flash ADC. Then, after having transferred to the PC's memory, each pulse was smoothed using the fast "zero area" digital filter, by means of the on line program. This algorithm produces a derived waveform, which has a zero value in the absence of peaks (signals) and has a shape similar to a smoothed second derivative in the regions where the peaks are present. The wide (more than few pulse widths) spectral structures are also removed from the waveform. This procedure is principally important because the base line of the detector output was strongly shifted by intense gamma flash from the neutron producing target. The program also creates pulse height and TOF spectra in the on line mode to monitor the data accumulation in real time. The raw data (input waveforms), as well as the TOF and pulse height spectra, were recorded on the hard disk of a PC.

The more elaborate off line analysis of the accu-

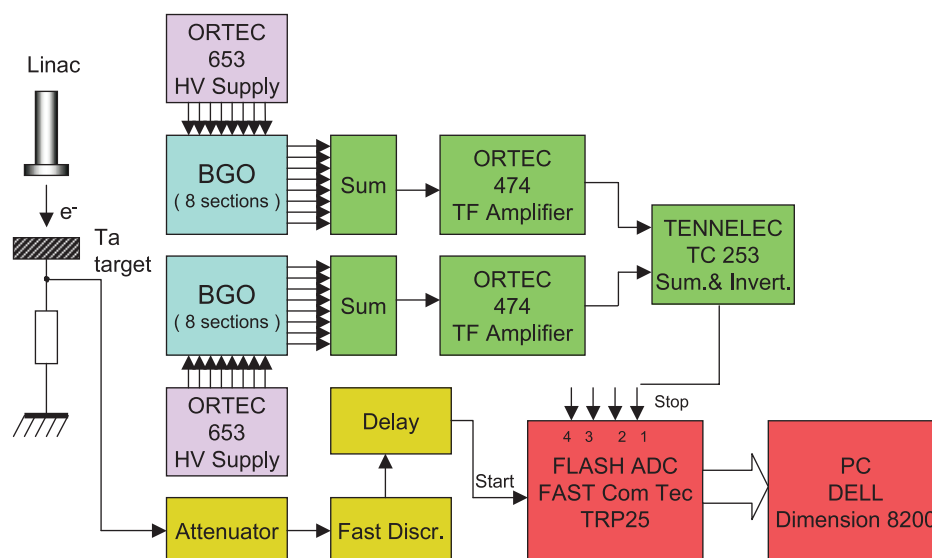


Fig. 6. Block diagram of the data taking system.

mulated raw data, including observation of the individual waveforms, was carried out in off line mode. The results of this analysis were stored in a 2 dimensional TOF  $\times$  pulse height matrix, which can be used subsequently to obtain TOF and pulse height spectra for arbitrary chosen amplitude or timing windows.

Fig. 7 shows the typical waveforms measured

with the  $^{137}\text{Cs}$  source, before and after the smoothing and filtering. The total number of the pulses in the waveform shown in Fig. 7(a) corresponds to the average input counting rate of  $\sim 29,000$  cps. Fig. 7(b) shows the stretched part of the input and derived waveforms, which includes a single pulse (with maximum at 10,247 ch) and two overlapping pulses (at 10,337 ch and 10,356 ch). In the derived

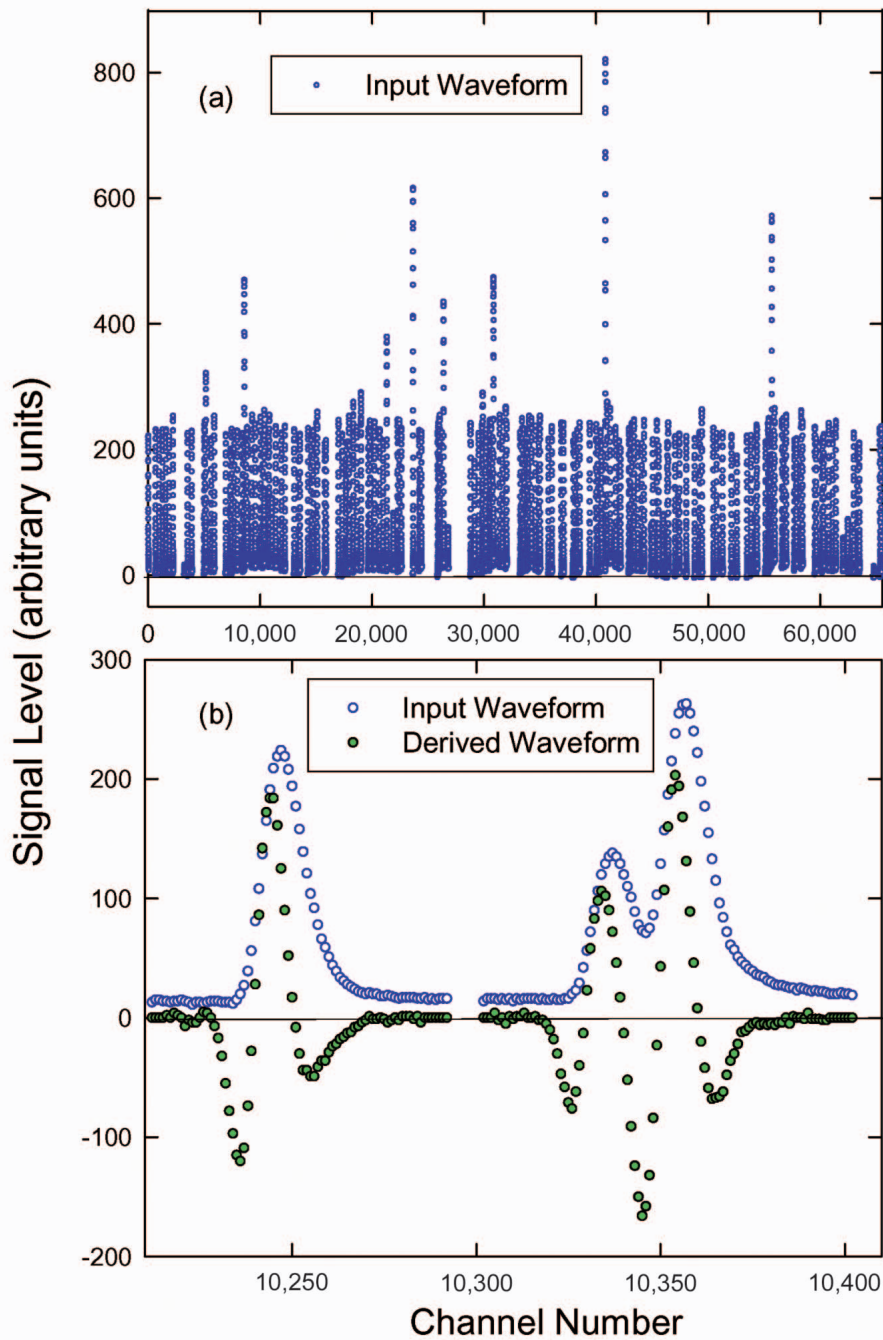


Fig. 7. A waveform of the BGO detector signal: (a) full-length input waveform (1  $\div$  65,536 channels); (b) stretched part (10,210  $\div$  10,410 channels) of the input and derived waveforms.

waveform, the base line fluctuates around the zero level, and derivatives of the overlapping pulses are separated enough to be treated as single pulses. The more sophisticated but time consuming procedure of the overlapping pulse deconvolution, such as the least squares fit, can be also applied.

### 3. EXPERIMENTAL RESULTS AND DISCUSSION

#### 3.1 BGO response function and efficiency

The main parameters of the BGO detector system, developed for the neutron capture cross section measurements by TOF method, were deduced from the experimental data and compared with the results of calculations.

The response function of BGO detector was measured using standard gamma ray sources  $^{137}\text{Cs}$  and  $^{60}\text{Co}$ . The gamma ray energy resolution of the whole 16 section detector measured with  $^{137}\text{Cs}$  (0.662 MeV) was about 15.5 %. Fig. 8 displays a response function measured with  $^{137}\text{Cs}$  source and that one calculated using the Monte Carlo code EGS4. For comparison with the measurement, the calculated pulse height distribution was corrected

for experimentally observed energy resolution. The efficiency of the whole detector,  $89.3 \pm 2 \%$  (at 80 keV discrimination level), obtained experimentally and corrected for the pulse pile up, was in a good agreement with the calculated value  $91.1 \pm 0.1 \%$ .

#### 3.2 Counting rates and TOF spectra

Figs. 9,10 show the time of flight spectra obtained with  $^{10}\text{B}$  and  $^{237}\text{Np}$  samples, respectively. Also shown are the energies of the filter resonance dips; notch resonances are marked with asterisks. For the  $^{10}\text{B}$  sample, spectra were obtained by reprocessing off line the raw waveform data at two discrimination levels, 360 keV (lower) and 600 keV (upper). This pulse height range was chosen to cover 480 keV gamma rays from  $^{10}\text{B}(n, \gamma)^7\text{Li}^*$  reaction, taking into account the energy resolution of the BGO detector,  $\sim 15 \%$  at 480 keV. The energy (TOF) dependence of the background was obtained by fitting the number of counts observed at notch resonance dips 336 eV (Mn), 132 eV (Co), 1.457 eV (In) and low energy range  $\sim 0.01$  eV. It

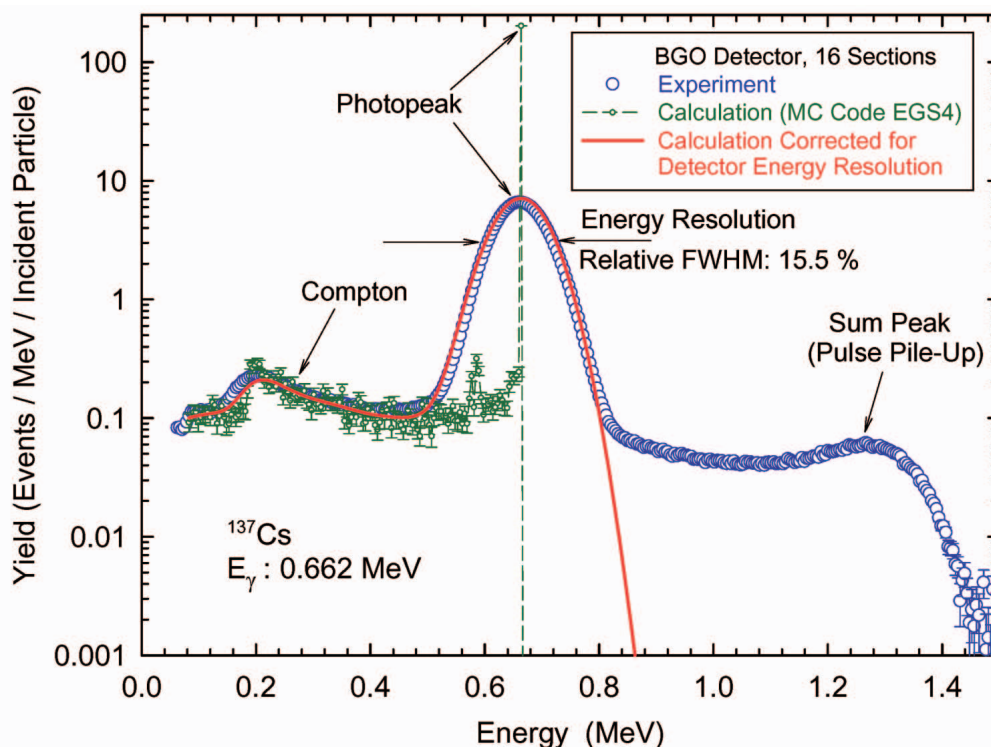


Fig. 8. Response function of the BGO detector (16 sections) for  $^{137}\text{Cs}$  gamma source: measured and calculated using a Monte Carlo code EGS4.

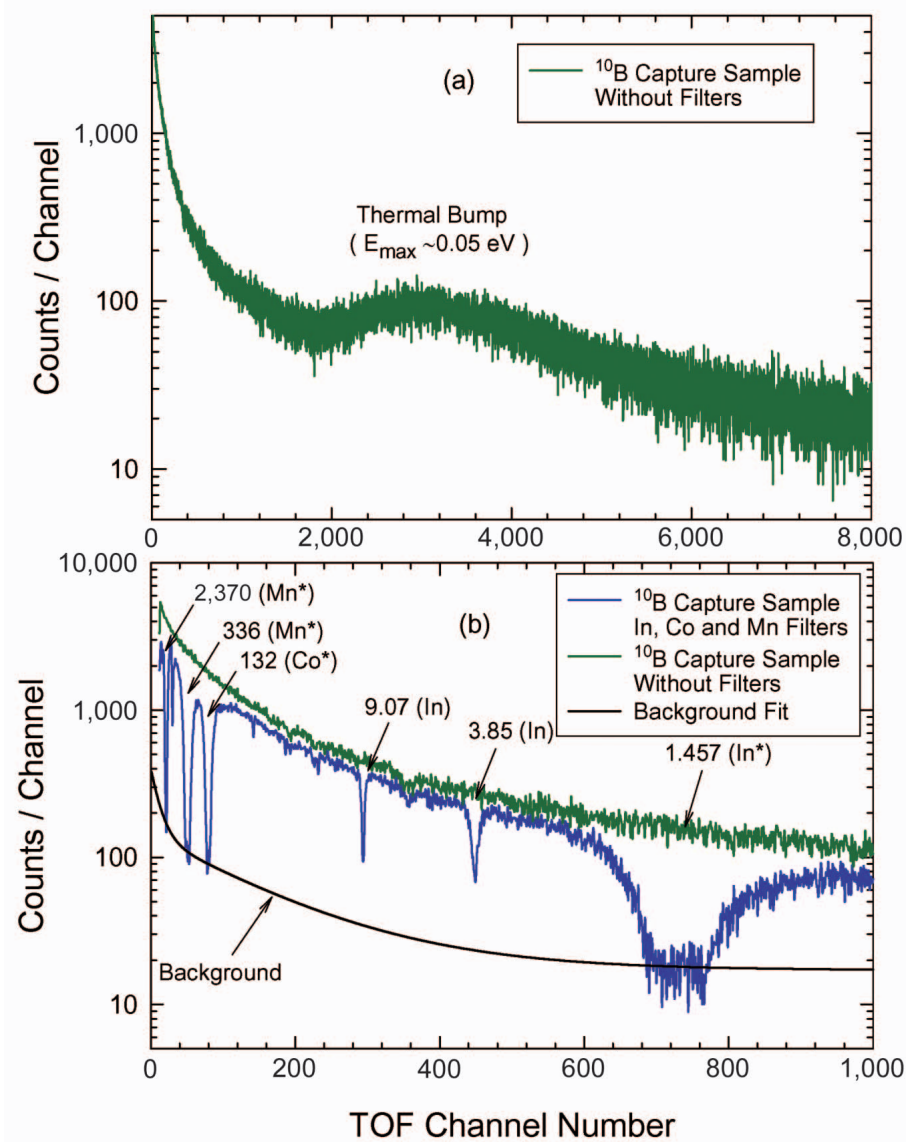


Fig. 9. The time-of-flight spectra of  $^{10}\text{B}$ : (a)  $^{10}\text{B}$  sample without filters, energy range  $0.011 \text{ eV} < E_n < 3 \text{ keV}$ ; (b)  $^{10}\text{B}$  sample with and without resonance filters of In, Co and Mn, fitted background, energy range  $1 \text{ eV} < E_n < 3 \text{ keV}$ . The energies of filter resonance dips are shown in eV, TOF channel width  $\Delta \text{ch} = 2 \mu\text{s}$ , Linac pulse width  $\Delta t_n = 3 \mu\text{s}$ .

was found that the relative background value was about 10 % in the energy range 1–400 eV, slowly increasing with a decrease in neutron energy.

For the case of  $^{237}\text{Np}$ , the natural radioactivity (26 Mbq) of the sample material led to very high time of flight independent background caused by 86.5 keV gamma rays from  $^{237}\text{Np}$ , and 300, 312 and 341 keV gamma rays from  $^{233}\text{Pa}$  (a daughter nucleus formed through  $\beta$  decay of  $^{237}\text{Np}$ ). To decrease this constant background, a 7 mm thick

cylindrical lead shield was inserted in the through hole of the detector. The raw data for  $^{237}\text{Np}$  have been reprocessed off line using the optimized values of 4.0 MeV and 6.0 MeV for lower and upper discrimination levels, respectively. The energy dependence of the background has been measured with a dummy sample, an empty thin walled Al container identical to that with  $^{237}\text{NpO}_2$  powder. Fig. 10 shows the TOF spectra for  $^{237}\text{Np}$  and dummy samples, as well as the differential spec-



trum obtained by subtraction of the evaluated background.

### 3.3 Neutron energy resolution

The neutron energy resolution is the most important parameter of the TOF facility. Making use of the formula (1), the relative neutron energy resolution can be written as:

$$\frac{\Delta E_n}{E_n} = \frac{2E_n^{1/2}}{\mu_0 L} \sqrt{(\Delta t)^2 + \frac{\mu_0^2}{E_n} (\Delta L)^2}, \quad (2)$$

where  $t$  is a quadratic sum of “pure” timing uncertainties like the fast neutron burst width  $\mu_n$ , the time channel width  $\mu_{ch}$ , and the time resolution of the electronics  $\mu_e$  and detector itself  $\mu_d$ , and  $L$  is a sum of “pure” geometrical uncertainties, such as the moderator thickness  $L_m$  and capture sample thickness  $L_d$ .

For the experimental evaluation of resolution function in the resonance energy range, it is convenient to approximate the resolution function of the TOF spectrometer by a Gaussian function:

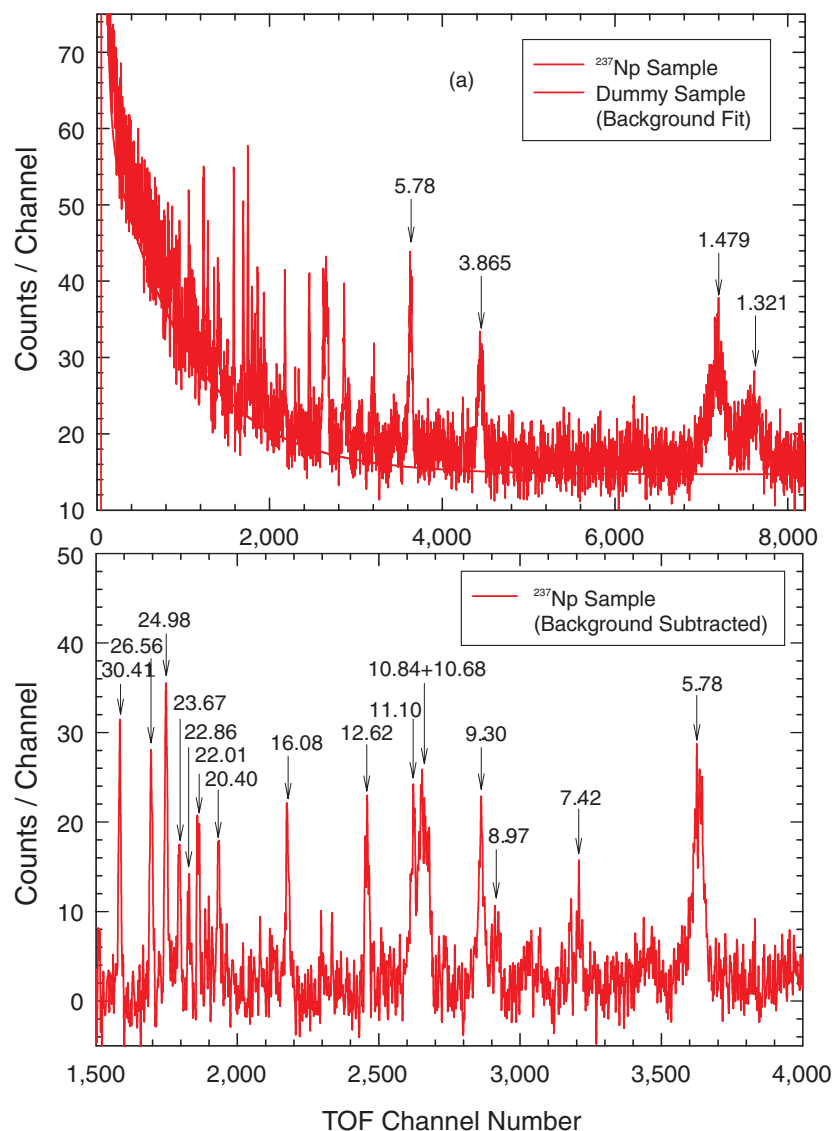


Fig. 10. The time-of-flight spectra of  $^{237}\text{Np}$ : (a) neptunium sample and dummy sample (background fit), energy range  $1.2 \text{ eV} < E_n < 3 \text{ keV}$ ; (b)  $^{237}\text{Np}$  sample (background subtracted),  $5 \text{ eV} < E_n < 32 \text{ eV}$ . The energies of some strongest resonances of  $^{237}\text{Np}$  are shown in eV, TOF channel width  $\mu_{ch} = 200 \text{ ns}$ , Linac pulse width  $\mu_n = 47 \text{ ns}$ .

$$R(E_n, E') = \frac{1}{W\sqrt{\pi}} \exp\left(-\frac{(E_n - E')^2}{W^2}\right) \quad (3)$$

The relation between the practically used quantity *FWHM* (full width of the resonance curve at half maximum) and parameter *W* is defined by the equation:

$$FWHM = 2W\sqrt{\ln 2} \quad (4)$$

The dispersion parameter *W* of the total resolution function can be written as a quadratic sum of four main components:

$$W^2 = W_D^2 + W_M^2 + W_T^2 + W_L^2 \quad (5)$$

where  $W_D$  is the Doppler broadening component,  $W_M$  is the moderator contribution,  $W_T$  and  $W_L$  are the totals of "pure" timing and geometrical uncertainties (as mentioned above), respectively. The Doppler broadening, which accounts for thermal movement of the sample atoms, is also included in resolution function.

For the 24.2 m flight path, the total relative en-

ergy resolution, as well as its components, is shown in Fig. 11 as a function of neutron energy from 0.01 eV to 10 keV. Also shown are relative half widths (FWHM) for resonances of  $^{237}\text{Np}$  calculated by convoluting the unbroadened capture cross sections with the Gaussian resolution function. They are compared with experimental values obtained by fitting the shape of the observed resonances of  $^{237}\text{Np}$  using the Gaussian function (3) for a short Linac pulse  $\tau_n = 100$  ns.

### 3.4 Gamma ray and neutron backgrounds

In the course of TOF measurement of neutron capture cross section, besides the prompt gamma rays the capture detector also registers background neutron and gamma ray radiation. Both backgrounds consist of a few components having TOF (neutron energy) dependent or independent intensity. Discussed below are those components which are associated directly with the developed gamma ray detector. These are the internal gamma ray background of BGO scintillator and

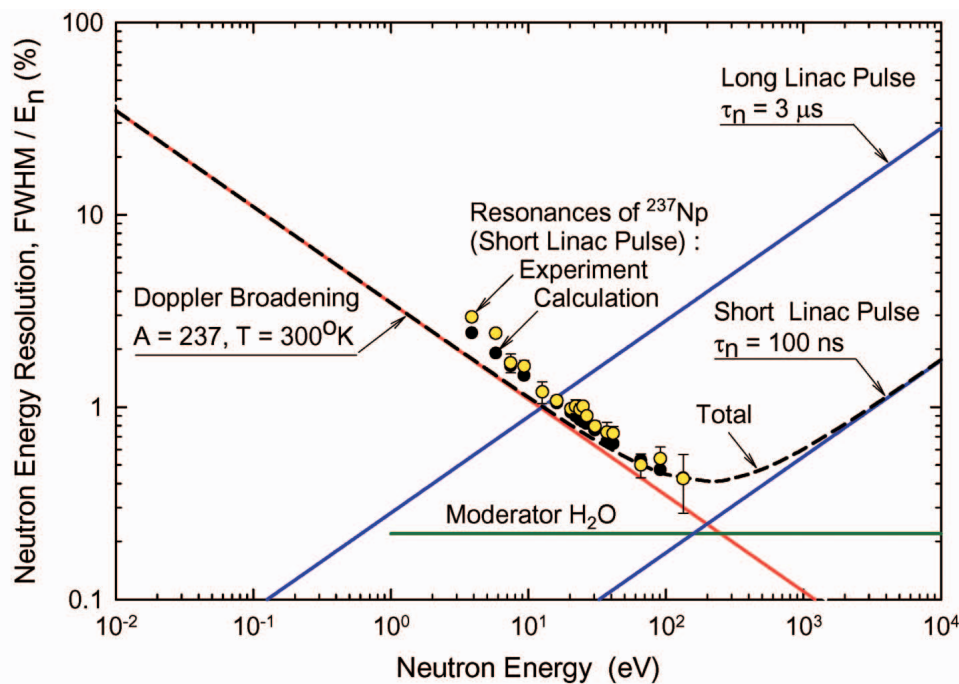


Fig. 11. The neutron energy resolution of the TOF spectrometer at 24.2 m flight path (relative FWHM) and its main components: Doppler broadening, moderator and "pure" timing uncertainties. Experimental points correspond to resonances of  $^{237}\text{Np}$  measured with short Linac pulse  $\tau_n = 100$  ns and channel width  $\tau_{ch} = 200$  ns.

the background caused by the beam neutrons scattered by the capture sample.

The natural gamma ray background of the described BGO detector is very low due to the use of specially purified materials. In the background pulse height distribution measured for bare (without any external shielding) detector shown in Fig.12, at least two gamma lines can be unambiguously identified. These are the 1.461 MeV line of  $^{40}\text{K}$  (room background) and the 2.614 MeV line (internal background caused by decay of  $^{212}\text{Po}$  impurity into  $^{208}\text{Tl}$ ). Also shown is an integral background counting rate for the whole BGO detector as a function of discrimination level. This component of the background is TOF independent and was measured both prior the experiment and during on beam capture measurements.

The gamma ray detector used for neutron capture cross section measurements should have low sensitivity to the neutrons scattered by the sample. The capture of such neutrons in the detector material causes background events, which can severely deteriorate accuracy of the measurement. For the case of BGO scintillator, this TOF depend-

ent background is mainly due to neutron capture by germanium nuclei. As a result, the energy dependence of sensitivity of the BGO detector to scattered neutrons reflects roughly the energy structure of a germanium capture cross section.

The neutron sensitivity of the bare BGO detector (without any internal neutron shield) was measured with the 3 mm thick graphite sample. In the energy range 1 1,000 eV this sample scatters about 11 % of the beam neutrons. The energy dependence of the sensitivity is shown in Fig. 13 as a function of neutron energy in the 1 1,000 eV range for two discrimination levels, 1 and 2 MeV. In order to decrease sensitivity of the present BGO detector to scattered neutrons with energies of 1 1,000 eV by at least 10 times, it would be necessary to use an internal neutron shield containing  $^6\text{Li}$  or  $^{10}\text{B}$ , which possess large absorption cross sections for thermal and slow neutrons. The level of discrimination between 1 and 2 MeV is adequate to eliminate gamma ray background of the detector itself and that of the radioactive sample, as well as the gamma rays caused by capture of scattered neutrons in the detector and neutron  $^{10}\text{B}$

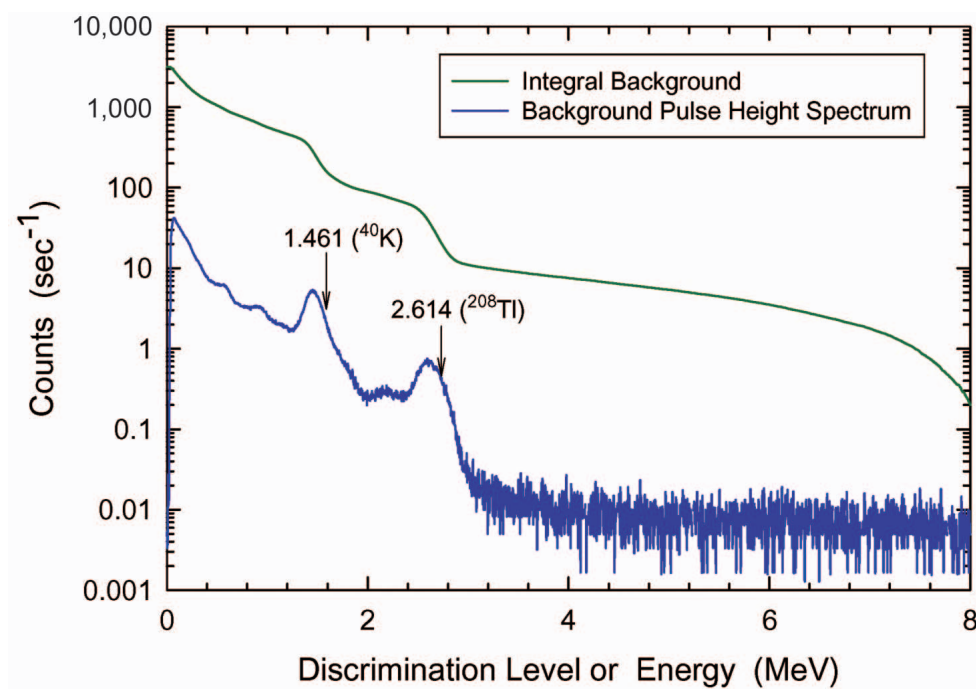


Fig. 12. The natural gamma background of the BGO detector without shielding: a pulse height distribution (solid, in counts / s · ch) and integral counting rate (dashed, in counts / s). The pulse height channel width is 4.12 keV.

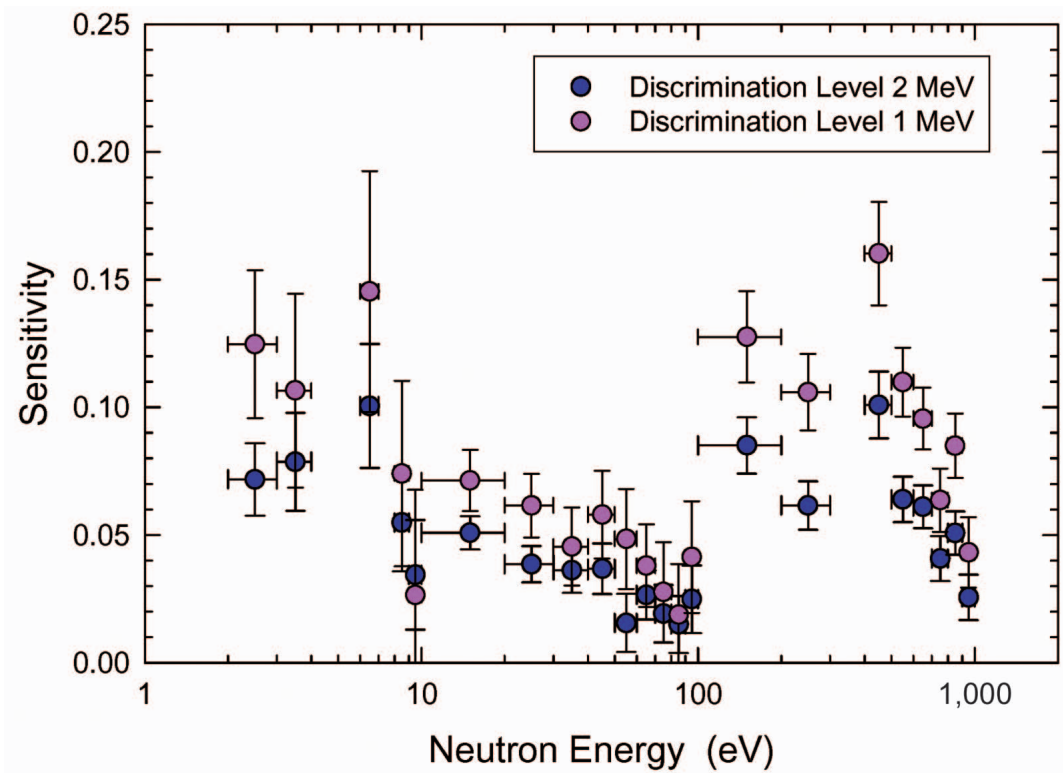


Fig. 13. The sensitivity of the BGO detector to neutrons scattered by the sample measured with different discrimination levels.

shield.

#### 4. SUMMARY

A new detector system that consists of the large BGO scintillation detector and associated flash ADC based data taking system was developed at the JNC for the measurements of neutron capture of radioactive nuclei by the time of flight method. The performance of the detector system was studied during the test measurements on a pulsed neutron beam at the KURRI Linac. The detector efficiency and response function, gamma ray and neutron energy resolution, background characteristics were experimentally obtained and compared with the results of calculations. The neutron capture reaction was studied with  $^{237}\text{Np}$  and  $^{10}\text{B}$  samples in the neutron energy range 1–1,000 eV. The results of tests show that this detector system can be effectively used for the measurements of neutron capture cross sections of radioactive nuclei by time of flight method from thermal to keV energy range.

#### ACKNOWLEDGEMENTS

The authors would like to express their sincere gratitude to the Administration of the Research Reactor Institute, Kyoto University for cooperation and making it possible to carry out measurements at the KURRI Linac. A help and participation of Prof. K. Kobayashi, S. Yamamoto, Samyol Lee and K. Takami in present research are highly appreciated.

The present investigation was carried in part within the framework of the JNC International Fellowship Research Program.

#### REFERENCES

- 1) O.A. Shcherbakov, " Present status of the measurements of nuclear data for transmutation ", Presentation at the Second Review Meeting for the JNC International Fellowship Program, O arai, October 18–19, 2001. JNC Report JNC TN1200 2001 004, December, p.217–230 (2001).
- 2) O.A. Shcherbakov, " Neutron capture cross section measurements by the TOF method ", Presentation at the Third Review Meeting for the JNC International Fellowship Program, Tokai, November 14–15, 2002.



- JNC Report JNC TN1200 2002 002, December, p.91  
108 (2002).
- 3 ) O. Shcherbakov, H. Harada, and S. Nakamura, “ Response functions of the multi sectional BGO gamma ray detector ”, Presentation at the 2002 Fall Meeting of the Atomic Energy Society of Japan, Iwaki, September 14 16, 2002. Abstracts, p.93.
  - 4 ) O. Shcherbakov, H. Harada, S. Nakamura, K. Furutaka and K. Kobayashi, “ Measurement of the neutron capture cross section of  $^{237}\text{Np}$  ”, Presentation at the 2003 Annual Meeting of the Atomic Energy Society of Japan, Sasebo, March 27 29, 2003. Abstracts, p.86.
  - 5 ) O.A. Shcherbakov, K. Furutaka, S. Nakamura, H. Harada and K. Kobayashi, “ A BGO detector system for studies of neutron capture by radioactive nuclides ”, to be published in Nuclear Instruments and Methods.